Dysregulation of renal sodium transporters in gentamicin-treated rats

MC Sassen[1,2,3], SW Kim[1,4], T-H Kwon[1,5], MA Knepper[6], RT Miller[7], J Frøkiær[1,8] and S Nielsen[1,2]

[1]*The Water and Salt Research Center, University of Aarhus, Aarhus C, Denmark;* [2]*Institute of Anatomy, University of Aarhus, Aarhus C, Denmark;* [3]*Philipps-University Marburg, Marburg, Germany;* [4]*Department of Internal Medicine, Chonnam National University Medical School, Gwangju, Korea;* [5]*Department of Biochemistry and Cell Biology, School of Medicine, Kyungpook National University, Taegu, Korea;* [6]*Laboratory of Kidney and Electrolyte Metabolism, National Heart, Lung, and Blood Institute, National Institutes of Health, Bethesda, Maryland, USA;* [7]*Nephrology Section, Case-Western Reserve University, Louis Stokes VAMC, Cleveland, Ohio, USA and* [8]*Institute of Clinical Medicine, Aarhus University Hospital, Aarhus N, Denmark*

We aimed to investigate the molecular mechanisms underlying the renal wasting of Na^+, K^+, Ca^{2+}, and Mg^{2+} in gentamicin (GM)-treated rats. Male Wistar rats were injected with GM (40 or 80 mg/kg/day for 7 days, respectively; GM-40 or GM-80). The expression of NHE3, Na–K-ATPase, NKCC2, ROMK, NCC, α-, β- and γ-ENaC, and CaSR was examined in the kidney by immunoblotting and immunohistochemistry. Urinary fractional excretion of Na^+, K^+, Ca^{2+}, and Mg^{2+} was increased and urinary concentration was decreased in both GM-40 and GM-80 rats. In cortex and outer stripe of outer medulla (cortex) in GM-80 rats, the expression of NHE3, Na–K-ATPase, and NKCC2 was decreased; NCC expression was unchanged; and CaSR was upregulated compared to controls. In the inner stripe of outer medulla (ISOM) in GM-80 rats, NKCC2 and Na–K-ATPase expression was decreased, whereas CaSR was upregulated, and NHE3 and ROMK expression remained unchanged. In GM-40 rats, NKCC2 expression was decreased in the cortex and ISOM, whereas NHE3, Na–K-ATPase, CaSR, ROMK, and NCC abundance was unchanged in both cortex and ISOM. Immunoperoxidase labeling confirmed decreased expression of NKCC2 in the thick ascending limb (TAL) in both GM-80- and GM-40-treated rats. Immunoblotting and immunohistochemical analysis revealed increased expression of α-, β-, and γ-ENaC in cortex in GM-80 rats, but not in GM-40 rats. These findings suggest that the decrease in NKCC2 in TAL seen in response to low-dose (40 mg/kg/day) gentamicin treatment may play an essential role for the increased urinary excretion of Mg^{2+} and Ca^{2+}, and play a significant role for the development of the urinary concentrating defect, and increased urinary excretion of Na^+ and K^+. At high-dose gentamicin, both proximal and TAL sodium transporter downregulation is likely to contribute to this.

Correspondence: *S Nielsen, The Water and Salt Research Center, Building 233/234, University of Aarhus, Aarhus C DK-8000, Denmark.*
E-mail: sn@ana.au.dk

Received 1 March 2005; revised 23 August 2005; accepted 5 October 2005; published online 19 July 2006

Kidney International (2006) **70,** 1026–1037. doi:10.1038/sj.ki.5001654; published online 19 July 2006

KEYWORDS: renal magnesium wasting; sodium transport; NKCC2; calcium-sensing receptor; nephrotoxicity; concentrating defect

Aminoglycoside antibiotics (AGAs) have been widely used clinically because of high efficacy and of low costs. AGAs, which include gentamicin, are used in the treatment of severe bacterial infections of the abdomen and urinary tract; however, serious problems and therefore dose-limiting factors are the side effects of nephrotoxicity and ototoxicity with an incidence up to 20% of patients undergoing treatment.[1,2] AGAs are low-protein binding drugs (<10%) and freely filtered through the glomerulus[3] without being metabolized in the body. About 10% of the parenterally administered drug accumulates in the renal cortex, leading to renal proximal tubule (PT) damage, including structural changes and functional impairment of the plasma membrane, mitochondria, and lysosomes.[4] After glomerular filtration, aminoglycosides are selectively retained in the epithelial cells of the PTs, specifically the S1 and S2 segments of the PT, but not in the distal parts of the nephron.[5,6]

Aminoglycoside-induced nephrotoxicity manifests clinically by nonoliguric renal failure with a progressive increase in serum creatinine levels and a decrease in urinary concentration after several days of administration. Moreover, AGAs can cause aminoaciduria, glucosuria, and increased urinary excretion of sodium, potassium, magnesium, and calcium.[7] In particular, dose-dependent hypermagnesiuria is known to occur soon after start of therapy and is reversible on discontinuation.[7,8] However, the underlying molecular mechanisms leading to renal wasting of sodium, potassium, magnesium, and calcium in response to gentamicin treatment are still undefined.

The main site for renal tubular sodium reabsorption is the PT, reabsorbing approximately two-thirds of the filtered sodium load. In this tubular segment, the type 3 Na^+/H^+ exchanger (NHE3) is mainly responsible for apical sodium

reabsorption,[9] and the type 2 Na-P_i cotransporter is also involved.[10,11] As in all renal tubule segments, the Na-K-ATPase is strongly expressed in the basolateral membrane[12] playing a crucial role for sodium reabsorption along the nephron. In the thick ascending limb (TAL), the bumetanide-sensitive Na–K–2Cl cotransporter (NKCC2),[13–15] NHE3 and Na–K-ATPase are the key sodium transporters for active sodium reabsorption. Potassium ions recirculate into the tubular lumen via the apical potassium channel Kir 1.1 (ROMK),[16,17] whereas chloride is reabsorbed basolaterally through ClC-Kb chloride channels.[18] Thus, NKCC2, ROMK, ClC-Kb, and Na-K-ATPase provide a lumen-positive transepithelial voltage in the TAL, which enhances magnesium and calcium reabsorption in this segment. In the distal convoluted tubule, the thiazide-sensitive Na–Cl cotransporter (NCC) is responsible for apical sodium reabsorption.[19,20] In the collecting duct, electrogenic entry of sodium from the lumen into the cells is mediated by ENaC located in the apical plasma membrane.[21] On the basolateral side, Na-K-ATPase transports sodium out of the cell into the extracellular interstitium and provides the driving force for sodium reabsorption. In rat kidney, three homologous subunits (α, β, and γ) contributing to the functional ENaC protein[22] are present in the late distal convoluted tubule, connecting tubule (CNT), cortical (CCD), and outer medullary collecting duct (OMCD), and to a lesser extent, in the inner medullary collecting duct.[23,24]

The kidney plays a key role in maintaining magnesium homeostasis. In the TAL, the main site of magnesium reabsorption along the nephron (reabsorbing approximately 70% of the filtered magnesium load), magnesium transport is passively driven by the lumen-positive voltage. Together with calcium, magnesium is reabsorbed paracellularly through the tight-junction protein paracellin-1.[25]

AGAs, which include gentamicin, function as polyvalent cations and activate the calcium sensing receptor (CaSR).[26] The CaSR is a large glycoprotein belonging to the superfamily of G protein-coupled receptors. In the TAL, the CaSR is highly expressed basolaterally,[27] sensing extracellular calcium, magnesium and other polyvalent cations, including AGAs. The localization of the CaSR in the kidney thus suggests that it may influence magnesium and calcium homeostasis by directly regulating renal magnesium and calcium reabsorption and excretion. In addition, there is evidence for a connection between divalent cation and water (and sodium) metabolism. Activation of the CaSR could impair sodium chloride and water reabsorption in the TAL and collecting duct by inhibition of hormone-stimulated cyclic adenosine 3′,5′ monophosphate (cAMP) formation and/or other calcium-dependent signaling mechanisms.[28,29]

The purposes of our present study were to identify the molecular mechanisms underlying the decreased urinary concentration and renal wasting of sodium, magnesium, and calcium associated with gentamicin-treatment. In particular, we test the hypothesis that gentamicin treatment induces downregulation of NKCC2, which in turn will reduce the lumen-positive transepithelial voltage in the TAL, leading to impaired passive paracellular reabsorption of magnesium and calcium in this part of the nephron. This hypothesis is consistent with the clinically and experimentally observed renal waste of magnesium and calcium in response to furosemide treatment.[30] To address this hypothesis, two protocols were used. In one protocol, a relatively high dose of gentamicin was used (80 mg/kg/day) known to be associated with PT defects evidenced by glucosuria. In the second protocol a moderate dose of gentamicin was used (40 mg/kg/day) which is known not to be associated with glucosuria but still leads to increased urinary excretion of Na^+, K^+, Ca^{2+}, and Mg^{2+} and urinary concentrating defects (both protocols). Specifically, we examined (1) whether there were changes in the abundance of the major renal sodium transporters along the nephron and collecting duct, that is, NKCC2, NHE3, Na–K-ATPase, NCC, and all ENaC subunits; (2) whether there were changes in the abundance of the ROMK and the calcium-sensing receptor, particularly in the TAL; and (3) whether these changes were associated with changes in urinary sodium, magnesium and calcium excretion, and urine concentration.

RESULTS

Gentamicin treatment decreases urinary concentration and increases urinary excretion of sodium, potassium, magnesium, and calcium

In both protocols (protocol 1, gentamicin 80 mg/kg/day and protocol 2, gentamicin 40 mg/kg/day), all gentamicin-treated rats exhibited significantly increased fractional excretions of sodium, potassium, magnesium, and calcium (Tables 1 and 2). Moreover, gentamicin-treated rats in both protocols demonstrated increased urine output and decreased urine osmolality (Tables 1 and 2), indicating decreased urinary concentration.

In protocol 1, at 24 h after the final injection of high-dose gentamicin, plasma trough levels of gentamicin $>0.5\,\mu$g/ml were measured. Gentamicin-treated rats presented massive glucosuria, whereas controls had no glucosuria. Rats treated with 80 mg/kg/day gentamicin also had polyuric renal failure with a threefold increase of plasma creatinine concentration along with significantly decreased renal creatinine clearance. Table 1 summarizes the functional data from protocol 1.

In protocol 2, there were no detectable plasma gentamicin trough levels 24 h after the final injection of the lower dose of gentamicin. Neither getamicin-treated nor control rats in protocol 2 had glucosuria. The gentamicin-treated rats exhibited significantly decreased creatinine clearance albeit at a lesser extent compared with protocol 1, whereas plasma creatinine levels were not significantly changed compared to controls. Table 2 summarizes the functional data from protocol 2.

Renal expression of NKCC2, NHE3, Na–K-ATPase, and NCC

We examined the renal abundance of the NKCC2 in gentamicin-treated rats and controls using protein samples

from the cortex or from the inner stripe of the outer medulla (ISOM) for semiquantitative immunoblotting. In protocol 1, NKCC2 expression of gentamicin-treated rats was significantly reduced in cortex to 51±7% of the control levels, $P<0.05$ (Figure 1a and b, Table 3) and also in ISOM to 57±7% of the control levels, $P<0.01$ (Figure 1c and d, Table 3). Accordingly, in protocol 2, NKCC2 abundance was decreased in cortex to 50±10% of the control levels, $P<0.05$ (Figure 1e and f, Table 4), and in ISOM to 60±10% of the control levels, $P<0.05$ (Figure 1g and h, Table 4) in rats treated with gentamicin.

Consistent with the immunoblotting data, immunohistochemical analysis of paraffin-embedded kidney sections revealed decreased immunoperoxidase labeling of NKCC2 in gentamicin-treated rats. In control rats (protocol 1), abundant immunoperoxidase labeling of NKCC2 was associated with apical plasma membrane domains of the cortical TAL (arrows in Figure 2a) and in the ISOM, strong NKCC2 labeling was observed in the apical plasma membrane domains of the medullary TAL (arrows in Figure 2c). In contrast, in gentamicin-treated rats (80 mg/kg/day of gentamicin) the labeling intensity of NKCC2 was markedly reduced both in cortical and medullary TAL (arrows in Figure 2b and d) as compared with controls (Figure 2a and c). Moreover, in protocol 2 (40 mg/kg/day of gentamicin), immunolabeling of NKCC2 was decreased in cortical and medullary TAL of gentamicin-treated rats (arrows in Figure 2f and h) compared with controls (arrows in Figure 2e and g).

Next, we investigated whether there were changes in the protein expression of the Na^+/H^+ exchanger NHE3 in cortex and ISOM. In protocol 1, semiquantitative immunoblotting revealed significant downregulation of NHE3 expression in cortex in gentamicin-treated rats to 57±5% of the control levels, $P<0.01$ (Figure 3a and b, Table 3), whereas the abundance of NHE3 in ISOM was not altered compared to controls (Table 3). In protocol 2, NHE3 protein abundance was unchanged in cortex (Figure 3c and d, Table 4) and ISOM (Table 4).

These findings were consistent with immunohistochemical analysis. In protocol 1, in the kidney cortex of control rats, immunoperoxidase labeling of NHE3 was associated with apical domains of the PTs (arrow in Figure 4a) and cortical TAL (asterisk in Figure 4a). Immunohistochemical analysis of the kidneys from gentamicin-treated rats revealed decreased labeling intensity of NHE3 in the PT (arrows in Figure 4b), whereas the labeling intensity was unchanged in the cortical TAL (asterisks in Figure 4b). Light microscopic examination demonstrated tubular damage and cell death in gentamicin-treated rats (protocol 1). Tubular necrosis was most pronounced in the convoluted parts of PT (Figures 2b and 4b), whereas it was less severe in the straight part of the PT (not shown). Necrotic cells were detached from the tubular basement membrane and were seen in the tubular lumen. Furthermore, disruption of the brush border (P in Figure 4b) and focal loss of individual tubular cells in the PT (P in Figure 4b) were also seen. In the ISOM of kidneys from control rats, NHE3 labeling was observed in the

Table 1 | Functional parameters from protocol 1 (gentamicin 80 mg/kg/day)

	GM (n=10)	Control (n=7)
P-gentamicin trough level (μg/ml)	2.5±0.5**	<0.5
U-Gluc-STIX (mmol/l)	22.2±2.3**	negative
Ccr (ml/min)	0.4±0.05**	1.2±0.1
UO (μl/min)	14.4±1.7**	6.9±1
P-Osm (mosm/kg H_2O)	316±2.3**	305±1.1
U-Osm (mosm/kg H_2O)	864±72**	2002±300
P-Cr (μmol/l)	109.6±12.2**	33.3±1.9
P-Na (mmol/l)	134.1±1.4	136.1±1.4
P-K (mmol/l)	4.3±0.1	4.0±0.2
P-Mg (mmol/l)	1.4±0.03**	1.1±0.05
P-total Ca (mmol/l)	2.7±0.02**	2.4±0.03
FE-Na (%)	1.8±0.2**	0.6±0.05
FE-K (%)	178.1±19.9**	66.8±6.8
FE-Mg (%)	23.9±4.6**	0.7±0.1
FE-Ca (%)	8.8±0.9**	0.4±0.1
U-Na/K	0.29±0.01	0.3±0.01

Ccr, creatinine clearance; FE-Ca, fractional excretion of calcium into urine; FE-K, fractional excretion of potassium into urine; FE-Mg, fractional excretion of magnesium into urine; FE-Na, fractional excretion of sodium into urine; GM, gentamicin; P-Cr, plasma creatinine; P-gentamicin trough level, plasma gentamicin level 24 h after last injection; P-K, plasma potassium; P-Mg, plasma magnesium; P-Na, plasma sodium; P-osm, plasma osmolality; P-total Ca, plasma total calcium; U-Gluc-STIX, urine glucose measured by urine STIX; UO, urine output; U-osm, urine osmolality; U-Na/K, urine Na/K ratio.
Values are expressed as mean±s.e. GM n=10, control n=7. These values are measured at the last day of the experiment (day 7).
**$P<0.01$ compared with controls.

Table 2 | Functional parameters from protocol 2 (gentamicin 40 mg/kg/day)

	GM (n=10)	Control (n=7)
P-gentamicin trough level (μg/ml)	<0.5	<0.5
U-Gluc-STIX (mmol/l)	Negative	Negative
Ccr (ml/min)	1.1±0.1**	1.4±0.04
UO (μl/min)	10.8±0.7**	7.2±0.7
P-Osm (mosm/kg H_2O)	303±1.4	302±1.5
U-Osm (mosm/kg H_2O)	1359±85**	2103±217
P-Cr (μmol/l)	33.7±3.8	24.4±0.6
P-Na (mmol/l)	135.9±0.4	135.3±0.6
P-K (mmol/l)	5.2±0.2**	6.3±0.2
P-Mg (mmol/l)	0.9±0.04	0.8±0.03
P-total Ca (mmol/l)	2.3±0.05	2.4±0.1
FE-Na (%)	0.8±0.06*	0.5±0.1
FE-K (%)	72.2±8.6**	29.8±6.1
FE-Mg (%)	15.4±1.1**	1.8±0.7
FE-Ca (%)	2.3±0.2**	0.7±0.2
U-Na/K	0.37±0.02	0.31±0.02

Ccr, creatinine clearance; FE-Ca, fractional excretion of calcium into urine; FE-K, fractional excretion of potassium into urine; FE-Mg, fractional excretion of magnesium into urine; FE-Na, fractional excretion of sodium into urine; GM, gentamicin; P-Cr, plasma creatinine; P-gentamicin trough level, plasma gentamicin level 24 h after last injection; P-K, plasma potassium; P-Mg, plasma magnesium; P-Na, plasma sodium; P-osm, plasma osmolality; P-total Ca, plasma total calcium; U-Gluc-STIX, urine glucose measured by urine STIX; UO, urine output; U-osm, urine osmolality; U-Na/K, urine Na/K ratio.
Values are expressed as mean±s.e. GM n=10, control n=7. These values are measured at the last day of the experiment (day 7).
*$P<0.05$, **$P<0.01$ compared with controls.

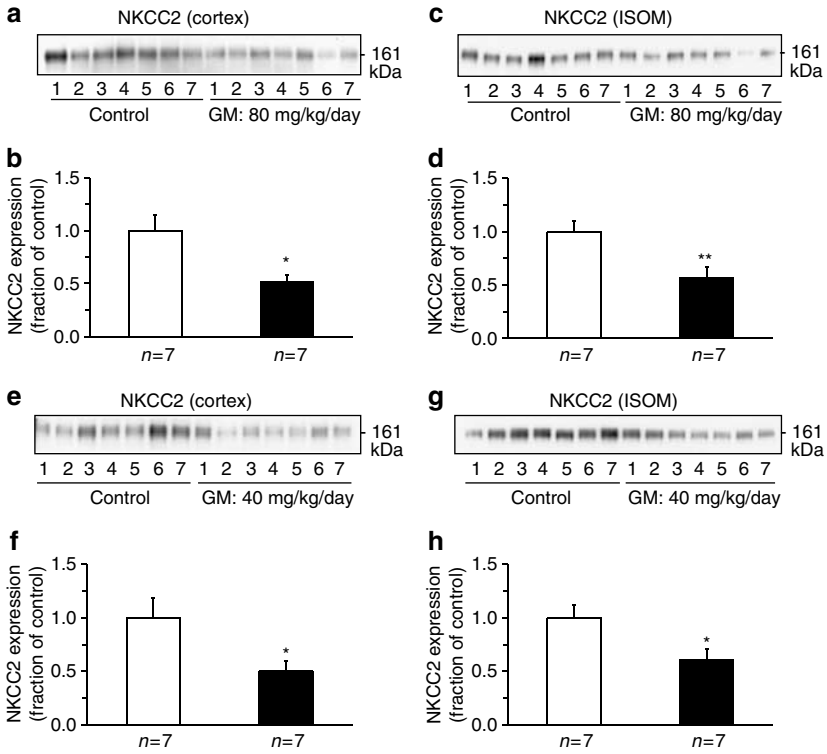

Figure 1 | Semiquantitative immunoblots of kidney proteins prepared from cortex, and ISOM from control and gentamicin-treated rats in protocol 1 (gentamicin 80 mg/kg/day) and protocol 2 (gentamicin 40 mg/kg/day). (**a**–**d**) In gentamicin-treated rats (protocol 1), NKCC2 protein abundance was markedly decreased in cortex and ISOM compared to controls. (**e**–**h**) In gentamicin-treated rats (protocol 2), NKCC2 protein abundance was significantly decreased in cortex and ISOM compared to control rats.

Table 3 | Densitometric analysis of protein expression in protocol 1 (gentamicin 80 mg/kg/day)

	GM (*n*=10)	Control (*n*=7)
Cortex		
NKCC2	51±7*	100±15
NHE3	36±4**	100±5
Na–K-ATPase	68±8*	100±8
NCC	88±24	100±8
CaSR	197±25**	100±13
α-ENaC	153±14**	100±8
β-ENaC	164±8**	100±4
γ-ENaC	197±11**	100±20
ISOM		
NKCC2	57±10**	100±9
NHE3	59±10	100±18
Na–K-ATPase	66±7**	100±5
ROMK	109±15	100±7
CaSR	160±18*	100±15
β-ENaC	179±15**	100±6
γ-ENaC	158±9**	100±9

CaSR, calcium sensing receptor; GM, gentamicin; NCC, thiazide-sensitive Na–Cl cotransporter; NHE3, type 3 Na/H exchanger; NKCC2, bumetanide-sensitive Na–K–2Cl cotransporter.
Values are expressed as mean±s.e.
*$P<0.05$, **$P<0.01$ compared with controls.

Table 4 | Densitometric analysis of protein expression in protocol 2 (gentamicin 40 mg/kg/day)

	GM-II (*n*=10)	Control (*n*=7)
Cortex		
NKCC2	50±10*	100±19
NHE3	86±13	100±8
Na–K-ATPase	136±20	100±9
NCC	89±5	100±6
CaSR	107±9	100±5
α-ENaC	110±16	100±11
β-ENaC	129±19	100±18
γ-ENaC	143±24	100±17
ISOM		
NKCC2	60±10*	100±11
NHE3	87±16	100±26
Na–K-ATPase	97±7	100±12
ROMK	78±23	100±18
CaSR	98±6	100±4
β-ENaC	173±9**	100±6
γ-ENaC	131±7**	100±6

CaSR, calcium sensing receptor; GM, gentamicin; NCC, thiazide-sensitive Na–Cl cotransporter; NHE3, type 3 Na/H exchanger; NKCC2, bumetanide-sensitive Na–K–2Cl cotransporter.
Values are expressed as mean±s.e.
*$P<0.05$, **$P<0.01$ compared with controls.

apical domains of the medullary TAL (T in Figure 4c) and thin limb structures. The immunolabeling intensity in the ISOM was unchanged in gentamicin-treated rats (Figure 4d) compared to controls.

Immunoblotting of the α_1-subunit of the Na-K-ATPase in cortex and ISOM revealed significant reduction in the expression in gentamicin-treated rats (protocol 1) to 68±8% of the control levels, $P<0.05$ (Figure 5a and b, Table 3) in

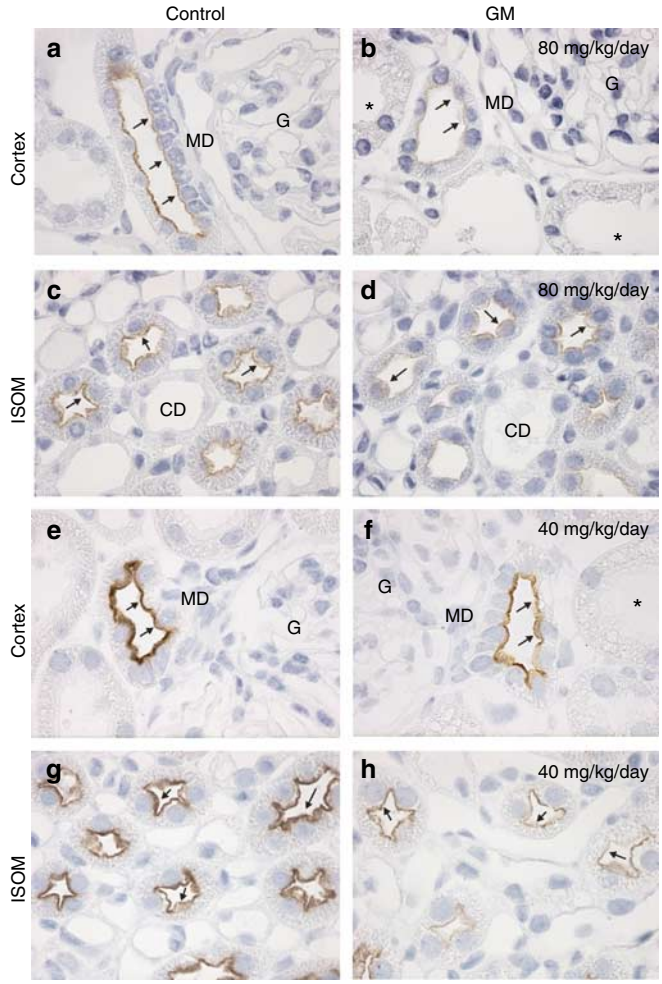

Figure 2 | Immunoperoxidase microscopy of NKCC2 in cTAL and mTAL in protocol 1 (gentamicin 80 mg/kg/day) and protocol 2 (gentamicin 40 mg/kg/day). In response to gentamicin, immunoperoxidase labeling of NKCC2 is decreased in cTAL (**b** and **f**, arrows) compared to controls (**a** and **e**, arrows) and mTAL (**d** and **h**, arrows) compared to controls (**c** and **g**, arrows). MD, macula densa; G, glomerulus; asterisk indicates PT (panel **b** and **f**) and arrows indicate NKCC2 labeling in cTAL and mTAL.

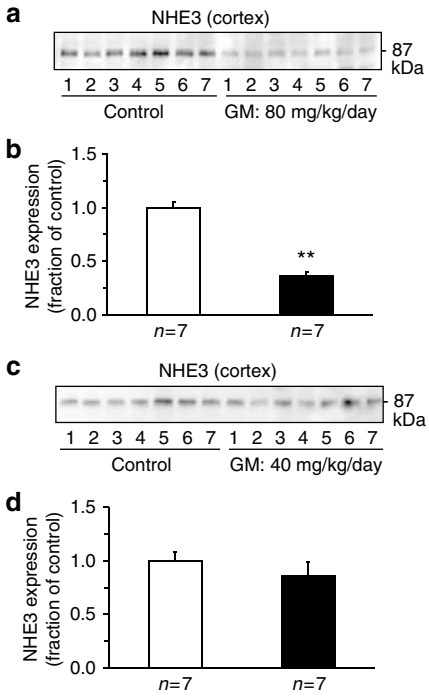

Figure 3 | Semiquantitative immunoblots of kidney proteins prepared from cortex from control and gentamicin-treated rats. (**a** and **b**) In protocol 1 (gentamicin 80 mg/kg/day), NHE3 protein abundance is reduced in response to gentamicin. (**c** and **d**) In protocol 2 (gentamicin 40 mg/kg/day), NHE3 expression remains unchanged.

cortex and 66±7%, $P<0.01$ in ISOM (Figure 5c and d, Table 3). In contrast, in protocol 2, the expression of the α_1-subunit of the Na–K-ATPase was not changed in cortex (Figure 5e and f, Table 4) or in ISOM (Figure 5g and h, Table 4).

Next, we examined the renal abundance of the NCC in gentamicin-treated rats and controls. In protocol 1 (Table 3) and protocol 2 (Table 4), NCC expression was unchanged in rats receiving gentamicin injections compared with controls.

Renal expression of ROMK

In the ISOM, we determined ROMK protein abundance by semiquantitative immunoblotting. ROMK expression was unchanged in rats treated with gentamicin compared to control rats in both protocol 1 (Table 3) and protocol 2 (Table 4).

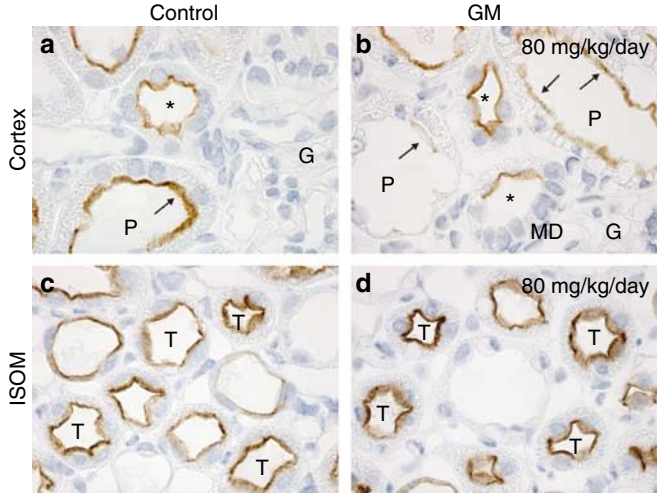

Figure 4 | Immunoperoxidase microscopy of NHE3 in PT, cTAL, and mTAL in rats treated with 80 mg/kg/day gentamicin and controls. In protocol 1, gentamicin treatment results in severe alterations in the morphology of the proximal tubule (P in panel **b**), as indicated by vacuolization and elimination of parts of the brush border, along with decreased immunoperoxidase labeling of NHE3 (**b**, arrows) compared with controls (panel **a**, P, arrow). In cTAL (panels **a** and **b**, asterisk), NHE3 immunolabeling remains unchanged. Also in mTAL, NHE3 immunolabeling is unchanged (T in panels **c** and **d**). MD, macula densa; G, glomerulus; P, proximal tubule; asterisk, cTAL; arrowheads indicate NHE3 labeling in PT.

Renal expression of CaSR

The protein abundance of the CaSR was determined in cortex and ISOM from kidneys of gentamicin-treated or control rats. In protocol 1, semiquantitative immunoblotting revealed markedly increased CaSR expression in gentamicin-treated rats to 197±25% of the control levels in cortex, $P<0.01$ (Figure 6a and b, Table 3), and also in ISOM to 160±18% compared with controls, $P<0.05$ (Table 3). In contrast, in protocol 2, CaSR protein abundance was unchanged in gentamicin-treated rats compared with controls in cortex (Figure 6c and d, Table 4) and ISOM (Table 4). Immunohistochemical analysis confirmed these results. Immunoperoxidase labeling was associated with basolateral domains in TAL (Figure 7a and b) and gentamicin treatment (protocol 1) was associated with increased immunoperoxidase labeling in cortical TAL (arrows in Figure 7b).

Renal expression of ENaC (α-, β-, and γ-subunit)

In protocol 1, α-ENaC abundance in cortex was significantly upregulated in gentamicin-treated rats to 153±14% of the control levels, $P<0.01$ (Figure 8a, Table 3). The β-ENaC-subunit protein abundance in cortex was significantly increased in response to gentamicin treatment to 164±8%, $P<0.01$ (Figure 8a, Table 3), as well as in ISOM to 179±15%, $P<0.01$ (Table 3). Finally, also γ-ENaC expression in cortex (85 kDa band) was markedly increased in gentamicin-treated rats to 197±11%, $P<0.01$ (Figure 8a, Table 3) and the 70 kDa band was invisible. Moreover, in ISOM, γ-ENaC expression (85 kDa band) was significantly increased in gentamicin-treated rats to 158±9% of the control levels, $P<0.01$ (Table 3), and the 70 kDa band was nearly invisible.

In protocol 2, there was no difference in α-ENaC expression in cortex between the gentamicin-treated group and the control group (Figure 8b, Table 4). Moreover, the abundance of β-ENaC and γ-ENaC was unchanged in cortex in gentamicin-treated rats compared with controls (Figure 8b, Table 4), whereas a significant increase was noted in ISOM of kidneys from gentamicin-treated rats for both β-ENaC (173±9%, $P<0.01$, Table 4) and γ-ENaC (131±7%, $P<0.01$, Table 4).

Immunohistochemical analysis of β-ENaC in protocol 1 revealed increased immunoperoxidase labeling in CNT, CCD, and OMCD in response to gentamicin treatment compared with controls (data not shown). In parallel, immunoperoxidase labeling of γ-ENaC in protocol 1 was more intense in CNT, CCD (Figure 9a–d), and OMCD (not shown) compared with controls.

DISCUSSION

In the present study, we demonstrated that gentamicin treatment of rats was associated with increased urinary excretion of sodium, potassium, magnesium, and calcium. Moreover, urinary concentration ability was significantly decreased in response to gentamicin treatment. Light microscopic examination demonstrated severe PT damage and cell death in gentamicin-treated rats in protocol 1

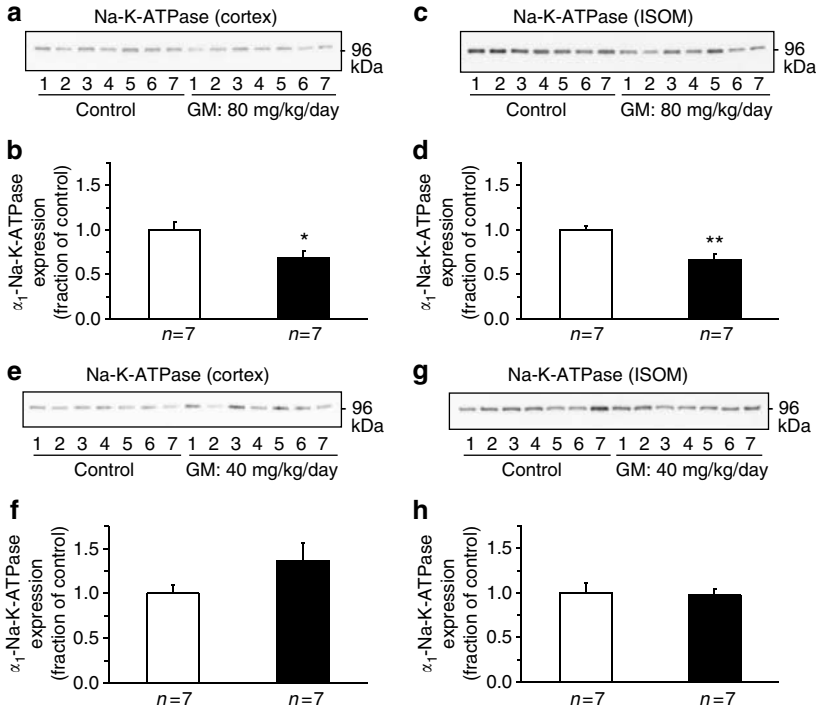

Figure 5 | Semiquantitative immunoblots of kidney proteins prepared from cortex, and inner stripe of outer medulla (ISOM) from control and gentamicin-treated rats. In protocol 1, 80 mg/kg/day gentamicin treatment leads to decreased Na-K-ATPase protein abundance in (**a** and **b**) cortex and (**c** and **d**) ISOM compared to controls. In protocol 2 (gentamicin 40 mg/kg/day), Na–K-ATPase expression was unchanged in (**e** and **f**) cortex and (**g** and **h**) ISOM.

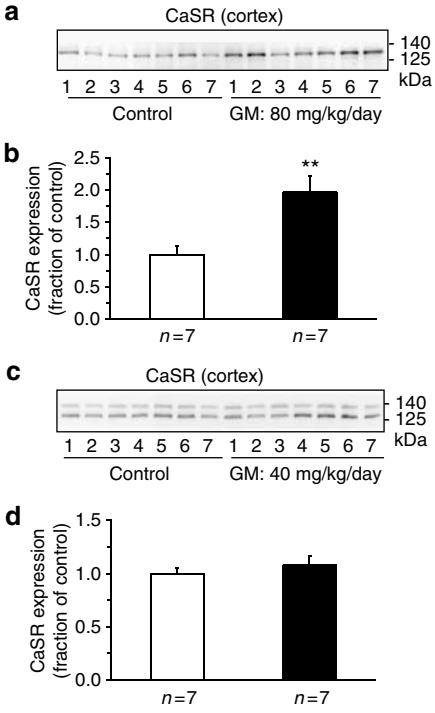

Figure 6 | Semiquantitative immunoblots of kidney proteins prepared from cortex from control and gentamicin-treated rats. In rats treated with 80 mg/kg/day gentamicin (protocol 1), CaSR protein abundance was increased in (**a** and **b**) cortex, but remained unchanged in (**c** and **d**) cortex in protocol 2, gentamicin 40 mg/kg/day.

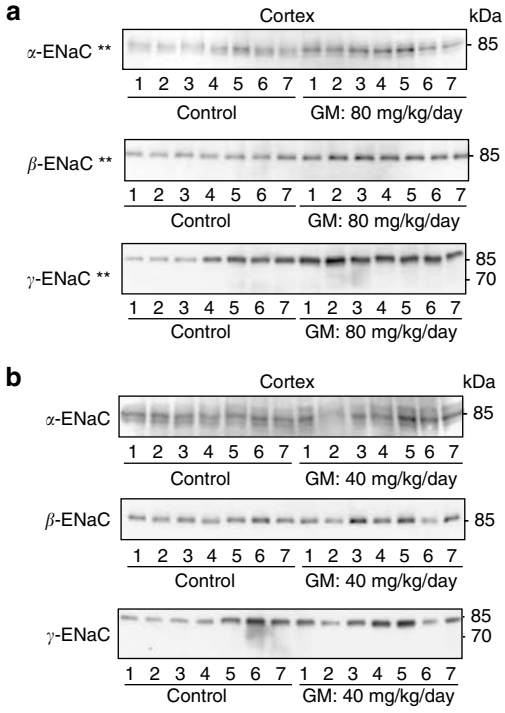

Figure 8 | Semiquantitative immunoblots of kidney proteins prepared from cortex from control and gentamicin-treated rats. (**a**) In protocol 1 (gentamicin 80 mg/kg/day), α-, β-, and γ-ENaC expression was significantly increased in gentamicin-treated rats. However, the 70 kDa band of γ-ENaC is nearly invisible, indicating low aldosterone activity. (**b**) In protocol 2 (gentamicin 40 mg/kg/day), α-, β-, and γ-ENaC expression was unchanged.

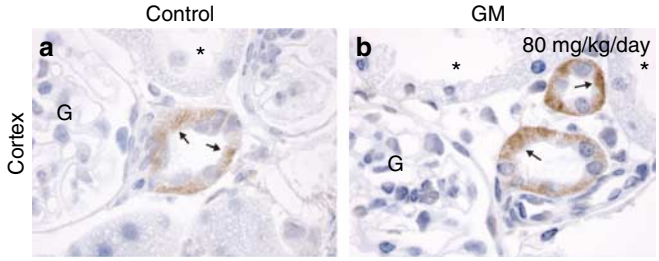

Figure 7 | Immunoperoxidase microscopy of CaSR in cTAL in kidneys from rats treated with 80 mg/kg/day gentamicin or controls. In response to gentamicin immunoperoxidase labeling of CaSR is increased (**b**, arrows) compared to controls (**a**, arrows). G, glomerulus; asterisk indicates PT and arrows indicate CaSR labeling in cTAL.

(80 mg/kg/day gentamicin) and the rats also developed glucosuria, consistent with previous studies. This was consistent with the observed decrease in the abundance of PT sodium transporters (NHE3, Na–K-ATPase). This was not seen by treatment with a relatively low dose of gentamicin (40 mg/kg/day). In high-dose gentamicin treatment the expressions of several TAL sodium transporters were reduced, whereas in low-dose gentamicin treatment NKCC2 abundance was selectively decreased. ENaC subunit expression was either unchanged or increased likely to represent a compensatory process. In conclusion, the decreased NKCC2 expression in the TAL is likely to contribute significantly to the urinary concentrating defect by impairing the generation of the hypertonic medullary interstitium. Importantly, this NKCC2 downregulation may also contribute significantly to the increased urinary magnesium and calcium excretion by decreasing the lumen-positive voltage. Also, the decreased abundance of PT sodium transporters and NKCC2 may contribute to the increased urinary sodium excretion. These conclusions will be discussed in detail in the followings.

Increased urinary excretion of sodium, potassium, magnesium, and calcium in response to gentamicin treatment in rats

Gentamicin-treated rats in both protocols presented with increased urinary excretion of sodium, potassium, magnesium, and calcium. We estimated this by increased fractional excretion of sodium, potassium, magnesium, and calcium. Consistent with this, it is well known that hypermagnesiuria seen in response to treatment with AGAs is always associated with hypercalciuria.[31,32] This suggests that AGAs inhibit renal tubular reabsorption of these two polyvalent cations in the TAL, where the filtered magnesium and calcium are mainly reabsorbed, and/or in the distal convoluted tubule.[33] We hypothesize that the decrease in the expression of NKCC2

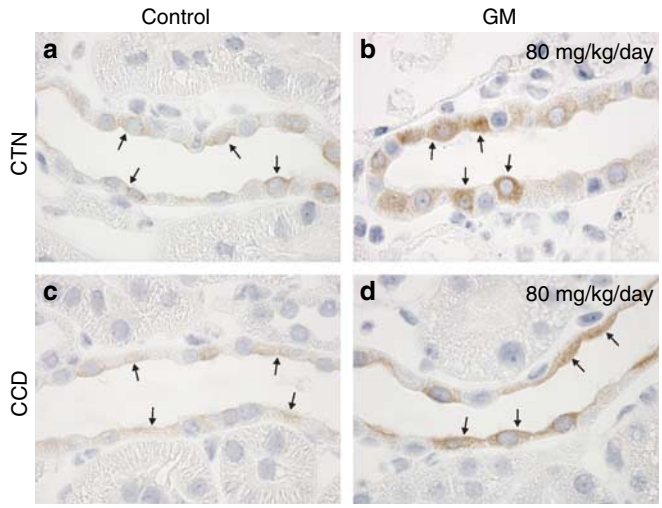

Figure 9 | Immunoperoxidase microscopy of γ-ENaC in the connecting tubule (CNT) and cortical collecting duct (CCD) in protocol 1. In rats treated with 80 mg/kg/day gentamicin, γ-ENaC immunoperoxidase labeling was increased in CNT (**b**, arrows) compared with controls (**a**, arrows) and CCD (**d**, arrows) compared with controls (**c**, arrows).

in TAL observed in gentamicin-treated rats may contribute to this, as this would lead to decreased sodium reabsorption in TAL and subsequently reduced lumen-positive voltage, as discussed below. Many studies have shown that renal wasting of magnesium, in addition to sodium, potassium, calcium, and phosphate wasting, occurs even by use of gentamicin in therapeutic doses, and is seen immediately after the infusion of the drug, and long before other evidence of renal dysfunction or structural injury develops.[8,34–36]

Dysregulation of renal sodium transporters and CaSR in TAL

We demonstrated that treatment with relatively high doses of gentamicin (protocol 1) was associated with significantly decreased protein abundance of NKCC2 and Na–K-ATPase in the TAL, whereas NHE3 and ROMK abundance was unchanged. In contrast, treatment with relatively low doses of gentamicin (protocol 2) was associated with selectively decreased abundance of NKCC2 in the TAL, but unchanged abundance of NHE3, Na–K-ATPase, and ROMK. As all gentamicin-treated rats in both protocols demonstrated significantly increased urinary excretion of sodium, it is therefore likely that the downregulation of NKCC2 may play a significant role in the decreased TAL sodium reabsorption and increased urinary excretion of sodium. Moreover, reabsorption of magnesium and calcium in the TAL may be decreased by impaired TAL sodium reabsorption resulting in a decreased lumen-positive voltage, and hence increased urinary magnesium and calcium excretion.

Activation of the CaSR has been shown to lead to an inhibition of passive reabsorption of magnesium and calcium in the TAL and reduced active transport in the distal convoluted tubule.[37–40] In addition, previous studies also indicate that activation of the CaSR increases both NaCl and calcium excretion in rats and humans.[39,41] The observed upregulation of the CaSR in rats treated with higher dose of gentamicin (protocol 1, 80 mg/kg/day) would be consistent with a role for the CaSR in mediating a decrease in NaCl reabsorption in the TAL and consequently a reduced reabsorption of divalent cations. Along with this view, we have previously demonstrated that CaSR expression was increased in experimentally induced hypercalcemia associated with decreased NaCl reabsorption and downregulation of NKCC2.[42] In agreement with the observed upregulation of CaSR in gentamicin-treated rats, previous studies have demonstrated that AGAs, which include gentamicin, have been shown to function as polyvalent cations activating the CaSR.[26]

Together with these previous findings, our results are consistent with the hypothesis that activation of the CaSR (e.g. viz. an increased expression) reduces the rate of sodium reabsorption in the TAL, thus decreasing the lumen-positive voltage. As the latter is the driving force for paracellular divalent cation transport in this nephron segment, this would consequently impair magnesium and calcium reabsorption.[43] Consistent with this, the use of loop diuretics causes renal wasting of magnesium and calcium associated with natriuresis. To date at least two second messenger system that can be activated by the CaSR are known to be involved in affecting sodium chloride transport in the TAL: (1) reduction of cellular cAMP and (2) activation of P_{450} and subsequent generation of 20-HETE.[44] In the TAL, NaCl, magnesium, and calcium reabsorption is likely to be cAMP-dependent. Thus, hormones that are known to increase cellular cAMP levels (e.g. AVP, PTH, glucagon, and calcitonin) increase NaCl, magnesium, and calcium reabsorption in the TAL.[45] Treatment with DDAVP (a vasopressin V_2-selective agonist) upregulates NKCC2 expression.[46,47] The V_2 receptor is linked to adenyl cyclase activation, and thus the increase of NKCC2 abundance by vasopressin might result from cAMP generation. Hence, in murine *SLC12A1* (mouse *NKCC2* gene) a cAMP-regulatory element was identified.[48] In addition, 20-HETE is known to inhibit NKCC2,[49] apical potassium recycling channels[50] and Na-K-ATPase,[51] thereby reducing sodium chloride reabsorption in the TAL. As an extension of these observations, patients with very potent activating mutations in the *CaSR* gene (causing autosomal dominant hypocalcemia, OMIM +601199) developed a Bartter-like phenotype. In addition to hypomagnesemia and hypocalcemia, these patients presented with renal salt and water loss associated with hypokalemic alkalosis.[52,53]

In protocol 1 and protocol 2, β- and γ-ENaC protein abundance was increased in ISOM. This is likely to reflect a compensatory effect in response to the decreased sodium reabsorption in the PT and TAL segments. However, unchanged urinary Na/K ratio[54] and unchanged NCC expression[20] indicate that the aldosterone-receptor was not activated in the animal models. Thus, further studies are needed to identify the underlying mechanisms for the observed changes of ENaC protein abundance.

Decreased urinary concentration in gentamicin-treated rats

Decreased urinary concentration was observed in response to gentamicin treatment. A previous study indicates that gentamicin treatment of rats reduces the expression of collecting duct AQP2 and AQP3 expression in rat kidney.[55] Interestingly, this study demonstrated that cAMP generation in response to AVP was decreased, but not in response to forskolin, suggesting that the primary impairment in the pathway of cAMP formation lies at the G protein level. In accordance with this gentamicin has been shown to impair cAMP generation in outer medullary TAL and collecting duct.[56] Whether such an inhibition could be potentially involved in the downregulation of NKCC2 remains to be demonstrated. However, it is likely that a downregulation of NKCC2 may reduce sodium chloride reabsorption in the TAL leading to a reduced countercurrent multiplication, and thus impair generation of hyperosmolar interstitium and urine concentration.

Dysregulation of renal sodium transporters and CaSR in cortex

Gentamicin is reabsorbed exclusively in the PT and accumulates in the renal cortex. In protocol 1, where rats received a higher dosage of gentamicin, expression of the PT sodium transporters, that is, NHE3, and Na-K-ATPase, and also NKCC2 were changed as determined by immunoblotting and in immunohistochemical analysis. Immunoperoxidase microscopy revealed that NHE3 expression was only decreased in the PT but unchanged in cortical TAL. Together with the significant glucosuria exclusively observed in rats treated with a higher dose of gentamicin, this indicates severe PT damage and suggests that this is very likely to be the reason for reduced NHE3 expression in the PT. In protocol 2, where rats received a lower dose of gentamicin, NKCC2 expression was selectively decreased in cortex observed by both immunoblotting and immunohistochemistry. NHE3 and Na–K-ATPase protein abundance remained unchanged.

In both protocols NCC expression was not changed, which is consistent with the previous functional data revealing absence of enhanced aldosterone action.[20] Moreover, in both protocols the urinary Na/K ratio was unchanged in rats receiving gentamicin compared to controls, which indicates that the aldosterone-receptor was not activated in the aldosterone-sensitive nephron segments. The results obtained regarding ENaC also support this view. Only in protocol 1, α-, β-, and γ-ENaC protein abundance was increased in contrast to protocol 2. The γ-ENaC 70 kDa band was nearly invisible, again indicating no increased aldosterone activity. The mechanisms underlying the increased ENaC expression are not clear.

CaSR protein abundance was increased in protocol 1, which might result from strong activation by gentamicin. The CaSR might play a role in impaired NKCC2 and Na–K-ATPase expression and NaCl reabsorption in the cortical TAL, followed by altered magnesium and calcium reabsorption. However, it is unclear whether downregulation of NKCC2 and Na-K-ATPase downregulation in cortex in protocol 1 resulted mainly from gentamicin toxicity or was mainly mediated by the influence of a strongly activated CaSR. Previous studies localized the CaSR also to the base of the apical brush-border membranes in the PT.[27] In addition, a recent study in opossum kidney (OK) cells (a PT cell line) and CaSR-transfected HEK-293 cells suggests that over-stimulation of the CaSR may contribute to AGA toxicity.[57] Immunohistochemistry in the present study shows CaSR protein expression exclusively in cortical and medullary TAL. However, this finding cannot exclude the localization and the functional role of CaSR in the PT and further studies are needed to establish this.

Conclusion

In gentamicin-treated rats (low dose of 40 mg/kg/day), the selective decrease in the expression of NKCC2 in the TAL may play a role for the urinary concentrating defect. As NKCC2 plays an important role in the reabsorption of sodium and maintaining the lumen-positive voltage in TAL, which is the driving force for passive magnesium and calcium reabsorption, the decreased NKCC2 expression following gentamicin treatment is likely to play a major role for the development of hypermagnesiuria and hypercalciuria. This is consistent with the clinically and experimentally observed renal waste of magnesium and calcium in response to furosemide treatment.

MATERIALS AND METHODS

Experimental protocols

The animal protocols have been approved by the boards of the Institute of Anatomy and Institute of Clinical Medicine, University of Aarhus according to the licenses for use of experimental animals issued by the Danish Ministry of Justice.

Protocol 1. Experiments were performed using male Hannover–Wistar rats (225–226 g, Møllegard Breeding Centre, Ry, Denmark). Starting with day 1, gentamicin ($n = 10$) was injected once a day intramuscularly over 7 days (1×80 mg/kg body weight/day, Hexamycin, Durascan Medical Products A/S, Odense, Denmark, Vnr. 089540). Control rats ($n = 7$) received vehicle alone (i.e., sterile 0.9% saline, intramuscularly). The rats were maintained on a standard rodent diet (Altromin No. 1324, Lage, Germany) and allowed free access to drinking water at all times. In the control group, rats were offered the amount of food corresponding to the mean intake of food consumed by gentamicin-treated rats during the previous day (pair-feeding). Thus, the food intake was matched between the two groups. The rats were maintained in metabolic cages during the entire experiment to determine 24 h urine output, water and food intake, and to allow urine collections for the measurements of Na^+, K^+, Cl^-, PO_4^{3-}, Mg^{2+}, total Ca^{2+}, creatinine, urea, osmolality, and glucose. The body weights were monitored. The rats were killed for immunoblotting and immunohistochemical studies 7 days after start of gentamicin treatment. The rats were anesthetized with isoflurane (Forane; Abbott Laboratories, Gentofte, Denmark) and a large laparotomy was made. Blood was collected from the inferior vena cava and analyzed for Na^+, K^+, Cl^-, PO_4^{3-}, Mg^{2+}, total Ca^{2+}, creatinine, urea, and osmolality. The right kidney was rapidly removed, dissected into zones cortex and

outer stripe of the outer medulla combined (cortex), ISOM, and inner medulla and processed for immunoblotting as described below. The left kidney was fixed by retrograde perfusion as described below.

Protocol 2. Another set of gentamicin-treated rats ($n = 10$) and control rats ($n = 7$) was made. In this protocol, the experimental settings were identical to protocol 1, except that gentamicin-treated rats were injected with a lower dose of gentamicin (1×40 mg/kg body weight/day, Hexamycin, Durascan Medical Products A/S, Vnr. 089540). Control rats ($n = 7$) received vehicle alone (i.e. sterile 0.9% saline, intramuscularly).

Clearance studies and urine glucose measurements

Clearance studies were performed over the last 24 h in protocol 1 and protocol 2. At the last day of each protocol, under isoflurane anesthesia, 2 ml of blood was collected into a heparinized tube for determination of plasma electrolytes and osmolality before the rats were killed. The plasma concentrations of sodium, potassium, magnesium, total calcium, and creatinine, and the urinary concentration of creatinine were determined (Vitros 950, Johnson & Johnson, Raritan, NJ, USA). The concentrations of urinary sodium, potassium, total calcium, and magnesium were determined by standard flame photometry (Eppendorf FCM6341, Eppendorf-Netheler-Hinz GmbH, Hamburg, Germany). The osmolality of the urine and plasma was determined by freezing-point depression (Advanced Osmometer, model 3900, Advanced Instruments, Norwood, MA, USA, and Osmomat 030-D, Gonotec, Berlin, Germany). Glucose levels in the urine were determined using a qualitative assessment by use of Multistix (Bayer, Bayer Denmark, Lyngby, Denmark).

Semiquantitative immunoblotting

The dissected renal cortex (which contains tissue from cortex and the outer stripe of the outer medulla), ISOM, and inner medulla were homogenized (Ultra-Turrax T8 homogenizer, IKA Labortechnik, Staufen, Germany) in ice-cold isolation solution containing 0.3 M sucrose, 25 mM imidazole, 1 mM ethylene diaminetetraacetic acid, 8.5 μM leupeptin, 1 mM phenylmethylsulfonyl fluoride, with pH 7.2. The homogenates were centrifuged at 4000 *g* for 15 min at 4°C to remove whole cells, nuclei, and mitochondria, the supernatant was pipetted off and kept on ice. The total protein concentration was measured (Pierce BCA protein assay reagent kit, Pierce, Rockford, IL, USA). All samples were adjusted with isolation solution to reach the same final protein concentrations and solubilized at 65°C for 15 min in sodium dodecyl sulfate-containing sample buffer, and then stored at −20°C. To confirm equal loading of protein, an initial gel was stained with Coomassie blue. Sodium dodecyl sulfate-polyacrylamide gel electrophoresis was performed on 9 or 12% polyacrylamide gels. The proteins were transferred by gel electrophoresis (BioRad Mini Protean II, Bio-Rad Laboratories GmbH, München, Germany) onto nitrocellulose membranes (Hybond ECL RPN3032D, Amersham Pharmacia Biotech, Little Chalfont, UK). The blots were subsequently blocked with 5% milk in PBS-T (80 mM Na_2HPO_4, 20 mM NaH_2PO_4, 100 mM NaCl, 0.1% Tween 20, pH 7.5) for 1 h and incubated overnight at 4°C with primary antibodies. The sites of antibody–antigen reaction were visualized with horseradish peroxidase-conjugated secondary antibodies (P447 or P448, diluted 1:3000; DAKO, Glostrup, Denmark) with an enhanced chemiluminescence system (ECL or ECL + plus) and exposure to photographic film (Hyperfilm ECL, Amersham Pharmacia Biotech, Little Chalfont, UK). To estimate the correct band size, we used a molecular weight marker (Precision Plus Protein Standards, All Blue, Catalog No. 161–0373, BioRad). The band densities were quantitated by scanning the films and normalizing the densitometric values. Results are presented as the relative abundances between the groups. ECL films with bands within the linear range were scanned using an AGFA scanner (ARCUS II). The labeling density was corrected by densitometry of Coomassie-stained gels run in parallel to the blotted gels.

Immunohistochemistry

A perfusion needle was inserted into the abdominal aorta of anesthetized rats and the vena cava was cut to establish an outlet. Blood was flushed from the kidneys with cold phosphate-buffered saline (PBS) (pH 7.4) for 15 s before switching to cold 3% paraformaldehyde in 0.1 M cacodylate buffer (pH 7.4) for 3 min. The kidney was removed and sectioned into 2–3 mm transverse sections and immersion fixed for additional 1 h, followed by 3×10 min washes with 0.1 M cacodylate buffer of pH 7.4. The tissue was dehydrated in graded ethanol and left overnight in xylene. After embedding in paraffin, 2 μm sections of the tissue were cut on a rotary microtome (Leica Microsystems A/S, Herlev, Denmark).

The sections were de-waxed with xylene and rehydrated with graded ethanol. Sections had endogenous peroxidase activity blocked with 0.5% H_2O_2 in absolute methanol for 10 min. In a microwave oven, the sections were boiled in target retrieval solution (1 mmol/l Tris, pH 9.0, with 0.5 mM ethylene glycol-bis (*b*-aminoethyl ether)) for 10 min. After cooling, nonspecific binding was blocked with 50 mM NH_4Cl in PBS for 30 min followed by 3×10 min with PBS blocking-buffer containing 1% bovine serum albumin, 0.05% saponin, and 0.2% gelatin. The sections were incubated with primary antibody (diluted in PBS with 0.1% bovine serum albumin and 0.3% Triton X-100) overnight at 4°C. The sections were washed 3×10 min with PBS wash-buffer containing 0.1% bovine serum albumin, 0.05% saponin, and 0.2% gelatin and incubated with horseradish peroxidase-conjugated secondary antibody (goat anti-rabbit immunoglobulin, DAKO A/S, Glostrup, Denmark) for 1 h at room temperature. After 3×10 min rinses with PBS wash-buffer, the sites with antibody–antigen reaction were visualized with a brown chromogen produced within 10 min by incubation with 0.05% 3,3′-diaminobenzidine tetrachloride (Kem-en Tek, Copenhagen, Denmark) dissolved in distilled water with 0.1% H_2O_2. Mayer's hematoxylin was used for counterstaining and after dehydration coverslips were mounted with hydrophobic medium (Eukitt, O Kindler GmbH & Co, Freiburg, Germany). Light microscopy was carried out with Leica DMRE (Leica Microsystems A/S, Herlev, Denmark). All the sections from the control and experimental group were processed and immunolabeled simultaneously.

Primary antibodies

Previously well-characterized rabbit polyclonal antibodies against the following renal sodium transporters were utilized: the NHE3,[58] the NKCC2 (BSC-1),[59] the thiazide-sensitive NCC (TSC),[20] and the ENaC subunits α-ENaC, β-ENaC, and γ-ENaC.[60] A mouse monoclonal antibody against CaSR was used.[61] A mouse monoclonal antibody against the Na-K-ATPase α1-subunit was kindly provided by Dr DM Fambrough, Johns Hopkins University Medical School.

Statistical analyses

Values were presented as means ± standard errors. Comparisons between two groups were made by unpaired *t*-test. *P*-values < 0.05 were considered significant.

ACKNOWLEDGMENTS

We thank Inger Merete Paulsen, Lotte Vallentin Holbech, Ida Maria Jalk, Gitte Kall, Helle Høyer, Zhila Nikrozi, Mette Vistisen, and Dorte Wulff for expert technical assistance. Martin C Sassen was supported by an EMBO short-term fellowship. The Water and Salt Research Center at the University of Aarhus is established and supported by the Danish National Research Foundation (Danmakrs Grundforskningsfond). The support for this study was provided by the WIRED program (Nordic Council and the Nordic Centre of Excellence Program in Molecular Medicine), Karen Elise Jensen Foundation, Human Frontier Science Program, the European Commission (QRLT 2000 00778 and QRLT 2000 00987), the Regional Technology Innovation Program of the MOCIE (RTI04-01-01, T-H Kwon), and the intramural budget of the National Heart, Lung, and Blood Institute, NIH.

REFERENCES

1. Bennett WM. Drug nephrotoxicity: an overview. *Renal Failure* 1997; **19**: 221–224.
2. Palmer BH, Heinrich WL. Toxic nephropathy. *Brenner & Rector's The Kidney*, 7th edn. 2003.
3. Kaloyanides GJ. Renal pharmacology of aminoglycoside antibiotics. *Contrib Nephrol* 1984; **42**: 148–167.
4. Mingeot-Leclercq MP, Tulkens PM. Aminoglycosides: nephrotoxicity. *Antimicrob Agents Chemother* 1999; **43**: 1003–1012.
5. Silverblatt FJ, Kuehn C. Autoradiography of gentamicin uptake by the rat proximal tubule cell. *Kidney Int* 1979; **15**: 335–345.
6. Vandewalle A, Farman N, Morin JP *et al.* Gentamicin incorporation along the nephron: autoradiographic study on isolated tubules. *Kidney Int* 1981; **19**: 529–539.
7. Alexandridis G, Liberopoulos E, Elisaf M. Aminoglycoside-induced reversible tubular dysfunction. *Pharmacology* 2003; **67**: 118–120.
8. Parsons PP, Garland HO, Harpur ES, Old S. Acute gentamicin-induced hypercalciuria and hypermagnesiuria in the rat: dose–response relationship and role of renal tubular injury. *Br J Pharmacol* 1997; **122**: 570–576.
9. Aronson PS. Role of ion exchangers in mediating NaCl transport in the proximal tubule. *Kidney Int* 1996; **49**: 1665–1670.
10. Biber J, Custer M, Magagnin S *et al.* Renal Na/Pi-cotransporters. *Kidney Int* 1996; **49**: 981–985.
11. Murer H, Forster I, Hilfiker H *et al.* Cellular/molecular control of renal Na/Pi-cotransport. *Kidney Int Suppl* 1998; **65**: S2–S10.
12. Kashgarian M, Biemesderfer D, Caplan M, Forbush III B. Monoclonal antibody to Na, K-ATPase: immunocytochemical localization along nephron segments. *Kidney Int* 1985; **28**: 899–913.
13. Ecelbarger CA, Terris J, Hoyer JR *et al.* Localization and regulation of the rat renal Na(+)-K(+)-2Cl- cotransporter, BSC-1. *Am J Physiol* 1996; **271**: F619–F628.
14. Nielsen S, Maunsbach AB, Ecelbarger CA, Knepper MA. Ultrastructural localization of Na–K–2Cl cotransporter in thick ascending limb and macula densa of rat kidney. *Am J Physiol* 1998; **275**: F885–F893.
15. Xu JC, Lytle C, Zhu TT *et al.* Molecular cloning and functional expression of the bumetanide-sensitive Na–K–Cl cotransporter. *Proc Natl Acad Sci USA* 1994; **91**: 2201–2205.
16. Giebisch G, Wang W. Potassium transport: from clearance to channels and pumps. *Kidney Int* 1996; **49**: 1624–1631.
17. Hebert SC, Wang WH. Structure and function of the low conductance KATP channel ROMK. *Wien Klin Wochenschr* 1997; **109**: 471–476.
18. Waldegger S, Jentsch TJ. From tonus to tonicity: physiology of CLC chloride channels. *J Am Soc Nephrol* 2000; **11**: 1331–1339.
19. Obermuller N, Bernstein P, Velazquez H *et al.* Expression of the thiazide-sensitive Na–Cl cotransporter in rat and human kidney. *Am J Physiol* 1995; **269**: F900–F910.
20. Kim GH, Masilamani S, Turner R *et al.* The thiazide-sensitive Na–Cl cotransporter is an aldosterone-induced protein. *Proc Natl Acad Sci USA* 1998; **95**: 14552–14557.
21. Duc C, Farman N, Canessa CM *et al.* Cell-specific expression of epithelial sodium channel alpha, beta, and gamma subunits in aldosterone-responsive epithelia from the rat: localization by *in situ* hybridization and immunocytochemistry. *J Cell Biol* 1994; **127**: 1907–1921.
22. Canessa CM, Schild L, Buell G *et al.* Amiloride-sensitive epithelial Na^+ channel is made of three homologous subunits. *Nature* 1994; **367**: 463–467.
23. Hager H, Kwon TH, Vinnikova AK *et al.* Immunocytochemical and immunoelectron microscopic localization of alpha-, beta-, and gamma-ENaC in rat kidney. *Am J Physiol Renal Physiol* 2001; **280**: F1093–F1106.
24. Schmitt R, Ellison DH, Farman N *et al.* Developmental expression of sodium entry pathways in rat nephron. *Am J Physiol* 1999; **276**: F367–F381.
25. Schlingmann KP, Konrad M, Seyberth HW. Genetics of hereditary disorders of magnesium homeostasis. *Pediatr Nephrol* 2004; **19**: 13–25.
26. McLarnon S, Holden D, Ward D *et al.* Aminoglycoside antibiotics induce pH-sensitive activation of the calcium-sensing receptor. *Biochem Biophys Res Commun* 2002; **297**: 71–77.
27. Riccardi D, Hall AE, Chattopadhyay N *et al.* Localization of the extracellular Ca^{2+}/polyvalent cation-sensing protein in rat kidney. *Am J Physiol* 1998; **274**: F611–F622.
28. Hebert SC, Brown EM, Harris HW. Role of the Ca(2+)-sensing receptor in divalent mineral ion homeostasis. *J Exp Biol* 1997; **200**: 295–302.
29. Sands JM, Naruse M, Baum M *et al.* Apical extracellular calcium/polyvalent cation-sensing receptor regulates vasopressin-elicited water permeability in rat kidney inner medullary collecting duct. *J Clin Invest* 1997; **99**: 1399–1405.
30. Quamme GA. Effect of furosemide on calcium and magnesium transport in the rat nephron. *Am J Physiol Renal Physiol* 1981; **241**: F340–F347.
31. Elliott WC, Patchin DS. Aminoglycoside-mediated calciuresis. *J Pharmacol Exp Ther* 1992; **262**: 151–156.
32. Keating MJ, Sethi MR, Bodey GP, Samaan NA. Hypocalcemia with hypoparathyroidism and renal tubular dysfunction associated with aminoglycoside therapy. *Cancer* 1977; **39**: 1410–1414.
33. Dai LJ, Ritchie G, Kerstan D *et al.* Magnesium transport in the renal distal convoluted tubule. *Physiol Rev* 2001; **81**: 51–84.
34. Foster JE, Harpur ES, Garland HO. An investigation of the acute effect of gentamicin on the renal handling of electrolytes in the rat. *J Pharmacol Exp Ther* 1992; **261**: 38–43.
35. Giapros VI, Cholevas VI, Andronikou SK. Acute effects of gentamicin on urinary electrolyte excretion in neonates. *Pediatr Nephrol* 2004; **19**: 322–325.
36. von Vigier RO, Truttmann AC, Zindler-Schmocker K *et al.* Aminoglycosides and renal magnesium homeostasis in humans. *Nephrol Dial Transplant* 2000; **15**: 822–826.
37. Bapty BW, Dai LJ, Ritchie G *et al.* Extracellular Mg2(+)- and Ca2(+)-sensing in mouse distal convoluted tubule cells. *Kidney Int* 1998; **53**: 583–592.
38. Bapty BW, Dai LJ, Ritchie G *et al.* Mg^{2+}/Ca^{2+} sensing inhibits hormone-stimulated Mg^{2+} uptake in mouse distal convoluted tubule cells. *Am J Physiol* 1998; **275**: F353–F360.
39. Hebert SC. Extracellular calcium-sensing receptor: implications for calcium and magnesium handling in the kidney. *Kidney Int* 1996; **50**: 2129–2139.
40. Kang HS, Kerstan D, Dai L *et al.* Aminoglycosides inhibit hormone-stimulated Mg^{2+} uptake in mouse distal convoluted tubule cells. *Can J Physiol Pharmacol* 2000; **78**: 595–602.
41. El-Hajj Fuleihan G, Seifter J, Scott J, Brown EM. Calcium-regulated renal calcium handling in healthy men: relationship to sodium handling. *J Clin Endocrinol Metab* 1998; **83**: 2366–2372.
42. Wang W, Li C, Kwon TH *et al.* Reduced expression of renal Na^+ transporters in rats with PTH-induced hypercalcemia. *Am J Physiol Renal Physiol* 2004; **286**: F534–F545.
43. Brown EM, Macleod RJ. Extracellular calcium sensing and extracellular calcium signaling. *Physiol Rev* 2001; **81**: 239–297.
44. Hebert SC. Calcium and salinity sensing by the thick ascending limb: a journey from mammals to fish and back again. *Kidney Int* 2004; **91**(Suppl): S28–S33.
45. de RC, Quamme G. Renal magnesium handling and its hormonal control. *Physiol Rev* 1994; **74**: 305–322.
46. Kwon TH, Nielsen J, Knepper MA *et al.* Angiotensin II AT1 receptor blockade decreases vasopressin-induced water reabsorption and AQP2 levels in NaCl-restricted rats. *Am J Physiol Renal Physiol* 2005; **288**: F673–F684.
47. Kim GH, Ecelbarger CA, Mitchell C *et al.* Vasopressin increases Na-K-2Cl cotransporter expression in thick ascending limb of Henle's loop. *Am J Physiol* 1999; **276**: F96–F103.
48. Igarashi P, Whyte DA, Li K, Nagami GT. Cloning and kidney cell-specific activity of the promoter of the murine renal Na–K–Cl cotransporter gene. *J Biol Chem* 1996; **271**: 9666–9674.
49. Amlal H, LeGoff C, Vernimmen C *et al.* Na(+)-K^+($NH4^+$)-$2Cl^-$ cotransport in medullary thick ascending limb: control by PKA, PKC, and 20-HETE. *Am J Physiol* 1996; **271**: C455–C463.

50. Wang WH, Lu M, Hebert SC. Cytochrome P-450 metabolites mediate extracellular Ca(2+)-induced inhibition of apical K^+ channels in the TAL. *Am J Physiol* 1996; **271**: C103–C111.
51. Escalante B, Erlij D, Falck JR, McGiff JC. Effect of cytochrome P450 arachidonate metabolites on ion transport in rabbit kidney loop of Henle. *Science* 1991; **251**: 799–802.
52. Vargas-Poussou R, Huang C, Hulin P *et al.* Functional characterization of a calcium-sensing receptor mutation in severe autosomal dominant hypocalcemia with a Bartter-like syndrome. *J Am Soc Nephrol* 2002; **13**: 2259–2266.
53. Watanabe S, Fukumoto S, Chang H *et al.* Association between activating mutations of calcium-sensing receptor and Bartter's syndrome. *Lancet* 2002; **360**: 692–694.
54. Bailey MA, Unwin RJ, Shirley DG. *In vivo* inhibition of renal 11beta-hydroxysteroid dehydrogenase in the rat stimulates collecting duct sodium reabsorption. *Clin Sci (London)* 2001; **101**: 195–198.
55. Lee J, Yoo KS, Kang DG *et al.* Gentamicin decreases the abundance of aquaporin water channels in rat kidney. *Jpn J Pharmacol* 2001; **85**: 391–398.
56. Kidwell D, Subramaniam S, Ott C, Jackson B. Impaired cyclic AMP generation in outer medullary tubules of gentamicin-treated rats. *Eur J Pharmacol* 1990; **191**: 489–492.
57. Ward DT, Maldonado-Perez D, Hollins L, Riccardi D. Aminoglycosides induce acute cell signaling and chronic cell death in renal cells that express the calcium-sensing receptor. *J Am Soc Nephrol* 2005; **16**: 1236–1244.
58. Fernandez-Llama P, Andrews P, Nielsen S *et al.* Impaired aquaporin and urea transporter expression in rats with adriamycin-induced nephrotic syndrome. *Kidney Int* 1998; **53**: 1244–1253.
59. Kim GH, Ecelbarger CA, Mitchell C *et al.* Vasopressin increases Na–K–2Cl cotransporter expression in thick ascending limb of Henle's loop. *Am J Physiol* 1999; **276**: F96–F103.
60. Masilamani S, Kim GH, Mitchell C *et al.* Aldosterone-mediated regulation of ENaC alpha, beta, and gamma subunit proteins in rat kidney. *J Clin Invest* 1999; **104**: R19–R23.
61. Awata H, Huang C, Handlogten ME, Miller RT. Interaction of the calcium-sensing receptor and filamin, a potential scaffolding protein. *J Biol Chem* 2001; **276**: 34871–34879.